Bulklike behavior of magnetoelasticity in epitaxial $Fe_{1-x}Ga_x$ thin films

M. Barturen,[1,2,3,4,5] D. Sander,[6] J. Milano,[2,3,5] J. Premper,[6] C. Helman,[7] M. Eddrief,[4,5] J. Kirschner,[6] and M. Marangolo[4,5]

[1]*Instituto de Tecnología, Universidad Argentina de la Empresa, Lima 775, (C1073AAO) Ciudad Autónoma de Buenos Aires, Argentina*

[2]*INN, CNEA-CONICET, Centro Atómico Bariloche, (R8402AGP) San Carlos de Bariloche, Argentina*

[3]*Instituto Balseiro, Universidad Nacional de Cuyo, Centro Atómico Bariloche, (R8402AGP) San Carlos de Bariloche, Argentina*

[4]*Sorbonne Université, CNRS, Institut des NanoSciences de Paris, UMR7588 F-75252, Paris, France*

[5]*Laboratoire International Franco-Argentin en Nanosciences, Unité mixte de Recherche du CNRS, de l'université Pierre et Marie Curie, Campus Boucicaut - 140, rue de Lourmel - 75015, Paris*

[6]*Max-Planck-Institut für Mikrostrukturphysik, Weinberg 2, D-06120 Halle, Germany*

[7]*CNEA, Centro Atómico Bariloche, (R8402AGP) San Carlos de Bariloche, Argentina*

(Received 25 March 2019; published 23 April 2019)

Bulk $Fe_{1-x}Ga_x$ alloys present a strong sensitivity of the magnetostrictive properties with Ga content with maximum magnetostriction near $x = 0.19$. Here, we present magnetoelastic coefficients measured by the cantilever method on $Fe_{1-x}Ga_x$ thin films grown by molecular beam epitaxy on GaAs(001). We find that Ga-dependent magnetoelastic coefficients in nanometer thin films are comparable in magnitude to the respective bulk values. Moreover, we compare thin films with a tetragonal structure due to a slightly preferential alignment of Ga pairs along the growth direction with and a cubic structure. It turns out that magnetoelastic coefficients are unaffected by a preferential alignment of Ga pairs along the growth direction.

DOI: 10.1103/PhysRevB.99.134432

I. INTRODUCTION

Magnetostriction of ferromagnetic materials describes the change of their shape or dimension in response to the reorientation of magnetization under the influence of an external magnetic field. This property is intensively exploited in modern technology and, more recently, in straintronic and sensor applications [1–3]. In the quest for new magnetostrictive materials, $Fe_{1-x}Ga_x$ (Galfenol) has attracted the attention of applied and fundamental investigation since, with a relative concentration of $x \sim 0.19$, it shows a magnetostriction twenty times higher than that of iron [4,5]. From a fundamental point of view, a debate is still open about the origin of enhanced magnetostriction. In particular, extrinsic factors were proposed to explain this phenomenon [6–8]. Nowadays it is believed to result from intrinsic factors; namely, the Ga-induced changes of the electronic structures [9–12]. Indeed, the large magnetostriction of $Fe_{1-x}Ga_x$ is stunning since magnetostriction originates from the strain dependence of the spin-orbit coupling (SOC), which is typically rather weak in $3d$ transition metals. It has been shown that Ga induces nonbinding Fe $3d$ states around the Fermi level. Consequently, enhanced magnetostriction is due to subtle modification of the density of states induced by Ga surrounding Fe atoms [10].

Previous experimental studies revealed that magnetostriction culminates for $x \sim 0.19$ and declines with the appearance of the Ga-ordered D03 cubic phase. The maximum magnetostriction can be slightly increased by a rapid quenching of the material that stabilizes the disorder A2 phase even at high x values. This scenario becomes more complex if we take also into account *ab initio* studies that reveal that the ordered B2 (the Ga atoms form Ga pairs) tetragonal structure (metastable) presents higher magnetostriction values [13]. These considerations suggest that Ga ordering may play a major role for a large magnetoelastic coupling. The primary objective of this paper is to present an experimental evaluation of the magnetoelastic coupling coefficients in $Fe_{1-x}Ga_x$ thin films and to study whether the magnetoelastic properties of $Fe_{1-x}Ga_x$ bulk are retrieved in thin films. Moreover, thin films open access to highly metastable configurations that can be stabilized by out-of-equilibrium growth: we were able to produce thin films presenting either the cubic structure or the tetragonally distorted B2-like phase for x ranging from 0.15 to 0.20. In Ref. [14], we show that the cubic structure is composed of tetragonal B2 grains with c axes (parallel to the Ga pairs) randomly oriented along the three spatial directions. On the other hand, the tetragonal structure occurs due to a spatial imbalance of the B2 grains, i.e., a larger fraction of Ga pairs along the growth direction. We determined the magnetoelastic coupling coefficients (MECs) in thin films with metastable configurations by means of the cantilever bending method and we compared the results with the corresponding bulk values. We found that the Ga pair orientation imbalance does not impact the MEC decisively and that bulk magnetoelastic properties are retrieved.

When it comes to magnetostriction in thin films it is necessary to recall that films are rigidly bonded to a substrate. When a magnetic field is applied, films are not free to change their length due to magnetization. Instead, magnetostrictive stress is present leading to curvatures of the sample [15]. The resulting curvature depends on the rigidity of the substrate. This is the reason why, in this case, the appropriate quantity to describe magnetostrictive properties is the magnetoelastic coupling, as explained in Refs. [16,17]. The MEC describe the strain dependence of the magnetic anisotropy energy (MAE) as it was established by Kittel 60 years ago [18]. It is known

that different factors can affect MEC in thin films: interface contributions, strain, and electronic structure effects [16].

From a structural point of view, $Fe_{1-x}Ga_x$ grown by MBE on ZnSe/GaAs(001) are characterized by metastable atomic structures. In Ref. [19] we show that a tetragonal structure can be stabilized by specific growth procedures. This distortion is attributed to Ga preferential ordering along the growth direction, i.e., the [001] direction. Indeed, x-ray diffraction experiments provide evidence for the presence of extra peaks due to a short-range ordering. These reflections are compatible with the presence of short-ranged B2 ordered regions in the sample [the $(\frac{1}{2}, \frac{1}{2}, \frac{1}{2})$ superlattice reflections of the DO3 phase are not detected]. Interestingly, the more stable cubic structure can be recovered by thermal annealing. This B2 ordering has noticeable consequences on the magnetic properties [20–22]; in particular, the induced spatial anisotropy is responsible for the perpendicular magnetic anisotropy observed in this system [14].

The formal description of the magnetoelastic free energy in tetragonal systems requires seven independent coefficients to describe it [17,23]. However, if we take into account that our experiment is sensible to the angle-dependent MEC, we arrive at a five-term description of the magnetoelastic energy for tetragonal systems:

$$\begin{aligned} U_{\rm me}^{\rm tet} = {} & B_1^{\perp}\left(\epsilon_{xx}\alpha_1^2 + \epsilon_{yy}\alpha_2^2\right) + B_1^{\parallel}\epsilon_{zz}\alpha_3^2 + B_1'\left(\epsilon_{xx}\alpha_2^2 + \epsilon_{yy}\alpha_1^2\right) \\ & + 4B_2^{\parallel}(\epsilon_{yz}\alpha_2\alpha_3 + \epsilon_{xz}\alpha_1\alpha_3) \\ & + 4B_2^{\perp}\epsilon_{xy}\alpha_1\alpha_2 + \cdots, \end{aligned} \tag{1}$$

where ϵ_{ii} refers to the strain in the i direction, ϵ_{ij} is the shear strain associated with directions ij, α_i represents the direction cosine of the magnetization associated with the i direction (where $i = 1, 2, 3$ corresponds to x, y, z, respectively). The dots indicate that higher-order terms are omitted, but may be important, e.g., in systems which are under significant epitaxial strain [16,24]. By considering $B_1 = B_1^{\perp} = B_1^{\parallel}$, $B_2 = 2B_2^{\perp} = 2B_2^{\parallel}$, and $B_1' = 0$, we retrieve the usual expression for cubic crystals:

$$\begin{aligned} U_{\rm me}^{\rm cub} = {} & B_1\left(\epsilon_{xx}\alpha_1^2 + \epsilon_{yy}\alpha_2^2 + \epsilon_{zz}\alpha_3^2\right) \\ & + 2B_2\left(\epsilon_{xy}\alpha_1\alpha_2 + \epsilon_{yz}\alpha_2\alpha_3 + \epsilon_{xz}\alpha_1\alpha_3\right) + \cdots. \end{aligned} \tag{2}$$

Very few MEC measurements have been reported for $Fe_{1-x}Ga_x$ thin films grown on GaAs(001) [25]. These experiments have been carried out with indirect techniques. The reported MEC values were very similar to the bulk ones, but they suffered from a large error margin. Our experiments provide quantitative data on MEC $B_{\rm i}$ from an analysis of the magnetization-induced magnetoelastic stress $\tau_{\rm me} = \frac{\partial U_{\rm me}}{\partial \epsilon}$. This magnetoelastic stress induces a curvature of a thin substrate-film composite, which changes upon an in-plane reorientation of the film magnetization direction. Thus the measurement of a curvature change upon magnetization reorientation gives access to the MEC.

In this work we measure the MEC of $Fe_{1-x}Ga_x$ epitaxial single-crystal thin films. We investigate two groups of samples, i.e., cubic and tetragonally distorted samples to study the role of strain in MEC. We present a systematic study of B_1 and B_2 as a function of Ga concentration x.

TABLE I. Structural parameters for the two groups of samples, cubic and tetragonal, and for the Fe pure sample as well. $V_{\rm cell} = ca^2$, calculated from the out-of-plane, c, and the in-plane, a, lattice parameters.

x	$V_{\rm cell}$(Å^3)	c/a	a (Å)
	Fe pure sample		
	23.4 ± 0.3	1.000 ± 0.005	2.86 ± 0.01
	Cubic $Fe_{1-x}Ga_x$ series		
0.14	24.0 ± 0.3	1.000 ± 0.005	2.88 ± 0.01
0.15	24.5 ± 0.3	1.003 ± 0.005	2.90 ± 0.01
0.25	24.8 ± 0.3	1.004 ± 0.005	2.92 ± 0.01
	Tetragonal $Fe_{1-x}Ga_x$ series		
0.14	24.1 ± 0.3	1.015 ± 0.005	2.87 ± 0.01
0.20	25.0 ± 0.3	1.010 ± 0.005	2.91 ± 0.01

II. EXPERIMENT

Epitaxial $Fe_{1-x}Ga_x$ films were deposited by molecular beam epitaxy on $c(2 \times 2)$ Zn-terminated ZnSe bilayers grown on GaAs(100). This system is a prototype of a low-reactive iron-semiconductor interface [26,27]. The samples were fabricated on ~100–150 μm thin substrates, where the low thickness facilitates the bending of the sample for the magnetoelastic curvature measurements. The films were covered by a protective gold capping layer of 5 nm thickness. Details of the growth are given in Ref. [19].

The films had a 75 nm nominal thickness and concentration x ranging from 0 to 0.25. By slight modifications of the thermal history of our samples, we succeeded in growing two groups of $Fe_{1-x}Ga_x$ thin films presenting cubic and tetragonal structures [19]. On the one hand, the as-grown samples present a tetragonal distortion of the film lattice in the growing direction that increases with Ga concentration. Such samples belong to the tetragonal series. On the other hand, some of them were annealed at 300 °C for few hours and, after that, they recovered the cubic structure observed in the bulk systems. They were labeled as cubic samples. The cubic structure can be stabilized also during growth by slight variations of the growth temperature in a very narrow temperature range.

The concentrations were determined by means of x-ray photoelectron spectroscopy (XPS) and confirmed by energy dispersive x-ray spectrometry (EDX). For an accurate evaluation of the thicknesses, x-ray reflectometry (XRR) experiments were carried out. To extract the lattice parameters, x-ray diffraction studies were performed by using Cu $K\alpha$ radiation in a Philips X'Pert MRD diffractometer. The results for the unit-cell volume ($V_{\rm cell}$) and c/a ratio, where c and a are the out-of-plane and in-plane lattice parameters, respectively, are shown in Table I.

A comparison between $V_{\rm cell}$ and Ga content x reveals that $V_{\rm cell}$ increases with x. The tetragonal samples are characterized by a c/a ratio in the range 1.001 to 1.0015.

The MEC is obtained from an analysis of the change in magnetization-induced curvature of a film-substrate composite. To this end an approximately 0.1-mm-thin rectangular substrate (10 mm long, 2.5 mm wide) is clamped along its

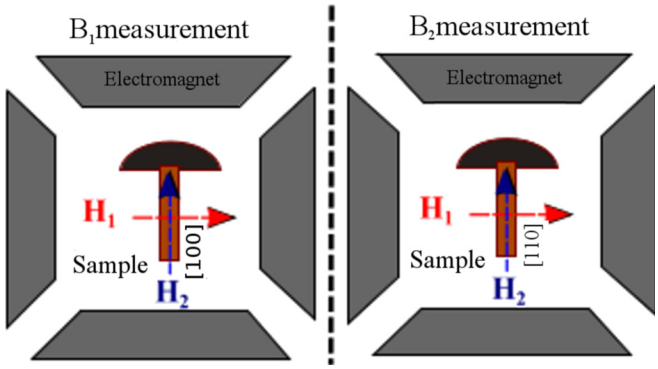

FIG. 1. MEC measurement setup. To measure B_1 the magnetic fields ($\mathbf{H}_1$ and $\mathbf{H}_2$) are applied along the [100] and [010] directions. To measure B_2 the magnetic fields ($\mathbf{H}_1$ and $\mathbf{H}_2$) are applied along the [110] and [1$\bar{1}$0] directions.

width at one end to a sample holder, while the other end is free. A sufficiently large length-to-width ratio of order 4 ensures free two-dimensional bending upon an in-plane reorientation of the film magnetization direction [16,23,28]. The film magnetization is kept at saturation in a single domain state, and the magnetization direction is varied from along the sample length to along the sample width by applying a sufficiently strong magnetic field (0.3 T) accordingly. See Fig. 1 for a sketch of the setup.

We use the deflection of two laser beams [29,30] which hit the sample surface at two points, top and bottom, separated along the sample length by l_{spot}. The beams are reflected from the sample surface onto two position-sensitive photodetectors at a distance l_{PD} from the sample surface. Thus, a sample curvature-induced deflection of the laser beams induces a laser spot displacement of Δ_{top} and Δ_{bottom} at the detectors. A reorientation of the magnetization M along the sample length and width induces a corresponding magnetoelastic stress change, and this induces a curvature change Δ_κ of the radius of curvature R which is calculated from the measured laser spot displacements:

$$\Delta_\kappa = \left(\frac{1}{R_{\text{length}}}\right)^{M_{\text{length}}} - \left(\frac{1}{R_{\text{length}}}\right)^{M_{\text{width}}} = \frac{\Delta_{\text{top}} - \Delta_{\text{bottom}}}{2 l_{\text{spot}} l_{\text{PD}}}. \quad (3)$$

TABLE II. Film (d_F) and substrate thickness (d_S).

x	d_F (nm)	d_S (μm)
	Pure Fe sample	
	55 ± 5	100 ± 10
	Cubic $Fe_{1-x}Ga_x$ series	
0.14	95 ± 5	130 ± 10
0.15	60 ± 5	130 ± 10
0.25	67 ± 5	130 ± 10
	Tetragonal $Fe_{1-x}Ga_x$ series	
0.14	75 ± 5	150 ± 10
0.20	73 ± 5	130 ± 10

TABLE III. Effective magnetoelastic coupling coefficients B^{eff} as determined from an in-plane magnetization reversal of a film with the given orientation and symmetry. The B_i are defined above in Eqs. (1) and (2). x_l is the sample length, and x_w is the sample width. See Ref. [23] for details.

Film structure	Film orientation	B^{eff}
Cubic	[100] $\parallel$ x_l, x_w	B_1
Tetragonal	[100] $\parallel$ x_l, x_w	$B_1^{\perp} - B_1'$
Cubic	[110] $\parallel$ x_l, x_w	B_2
Tetragonal	[110] $\parallel$ x_l, x_w	$2B_2^{\perp}$

This curvature change is caused by the magnetization-induced magnetoelastic stress change, and it corresponds to an effective MEC B^{eff} [16] of

$$B^{\text{eff}} = \frac{Y_S d_S^2}{6(1+\nu) d_F} \Delta_\kappa, \quad (4)$$

where Y_S, ν_S, d_S are Young's modulus, the Poisson ratio, and the thickness of the sample, respectively, and the film thickness is given by d_F. Data for film and substrate thickness are given in Table II. Note that the elastic properties of the GaAs substrate are directional dependent, and we use for sample length along $\langle 100 \rangle$ directions: $Y_S = 85.3$ GPa, $\nu_S = 0.312$ and for sample length along $\langle 110 \rangle$ directions: $Y_S = 121.3$ GPa, $\nu_S = 0.021$ [31].

The symmetry of the film materials and its crystallographic orientation with respect to the sample length and width determine which magnetoelastic coupling coefficients contribute to B^{eff} [16,23]. The curvature measurements are performed along the sample length. For films of cubic symmetry with the sample length parallel to $\langle 100 \rangle$, $B^{\text{eff}} = B_1$, and with the

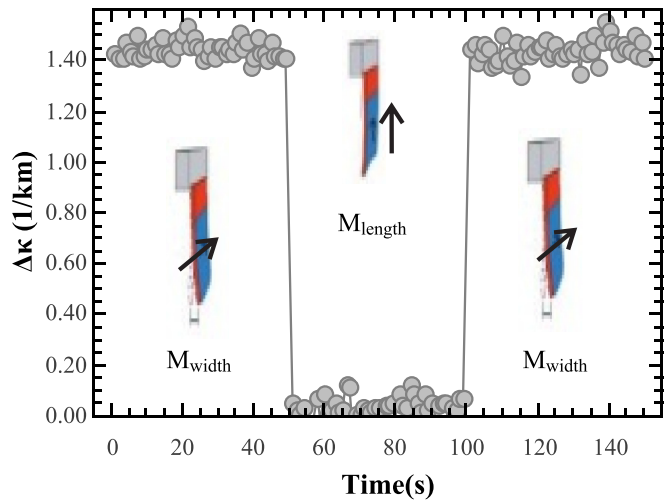

FIG. 2. Curvature signal from a typical cycle of 50 s of magnetic field along the width, then 50 s along the length and, finally, another 50 s along the width. M is the magnetization and the subscripts *width* and *length* indicate the magnetization direction. The measurements were taken for a tetragonal sample of $x = 0.20$ having the [100] direction along the cantilever length. The film thickness is (73 ± 5) nm. This curvature change indicates $B^{\text{eff}} = (-10 \pm 2)\,\text{MJ/m}^3$.

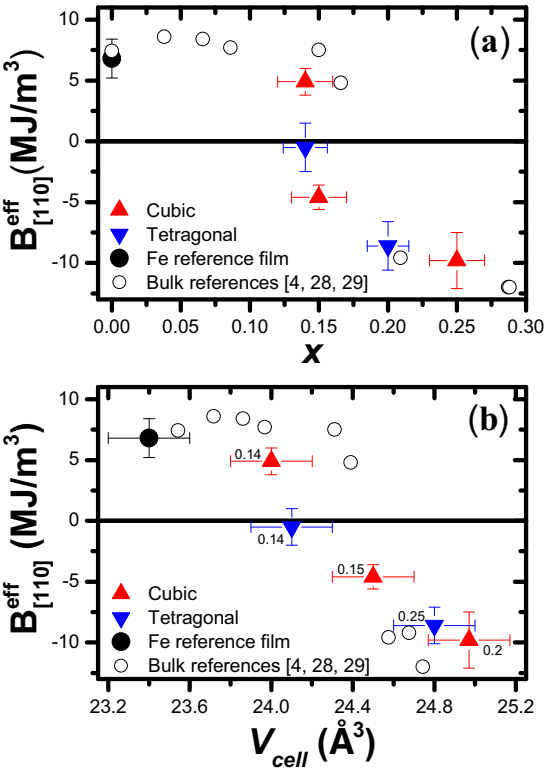

FIG. 3. B^{eff} measurements with $\mathbf{H}_1$ applied along [110] for cubic and tetragonal samples as a function of (a) x, and (b) V_{cell}, in which each experimental point is labeled with its respective x. Bulk references have been extracted from Refs. [4,32,33].

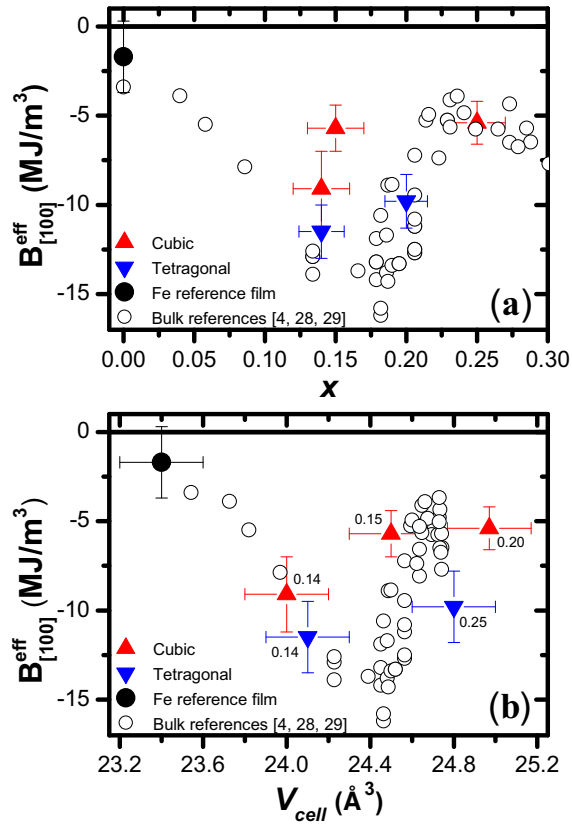

FIG. 4. B^{eff} measurements with $\mathbf{H}_1$ applied along [100] for cubic and tetragonal samples as a function of (a) x, and (b) V_{cell}, in which each experimental point is labeled with its respective x. Bulk references have been extracted from Refs. [4,32,33].

sample length along ⟨110⟩, $B^{\text{eff}} = B_2$. These relations for cubic and tetragonal symmetry are summarized in Table III.

III. RESULTS

Figure 2 shows an example of the obtained experimental data for the change of curvature for a cycle in which the magnetic field is applied 50 s in each direction, for a tetragonal sample of $x = 0.20$.

Figures 3(a) and 3(b) show the results for B^{eff} where the film direction [110] is along the cantilever length, $B^{\text{eff}}_{[110]}$, as a function of x and V_{cell}, respectively, for the two series. Bulk reference data are given for comparison [4,32,33]. The first important result is that the epitaxial thin films present $B^{\text{eff}}_{[110]}$ coefficients very similar to the respective bulk counterpart. The variation of $B^{\text{eff}}_{[110]}$ as a function of x follows the bulk trend [Fig. 3(a)].

The comparison of the MEC of the tetragonal samples with the cubic ones in Fig. 3 resembles largely similar data. Our major result is that the change in sign that occurs in bulk material for a Ga concentration of ∼0.17, also happens in our thin films but for a concentration slightly lower at ∼0.14. This difference could be ascribed either to a systematic error in the alloy composition (2%–3% by EDX) or to a different atomic structure of the thin film with respect to the bulk samples. We plot the same data as a function of V_{cell} [Fig. 3(b)]. We find a similar behavior with respect to $B^{\text{eff}}_{[110]}$ vs x, where a slight shift is still observed.

Figure 4(a) shows the results for $B^{\text{eff}}_{[100]}$ together with some B_1 bulk references [4,32,33]. To calculate the bulk references, the magnetostriction values given in Ref. [34] were multiplied by the difference of elastic constants as $B_1 = -\frac{3}{2}\lambda_{100}(c_{11} - c_{12})$. To obtain $(c_{11} - c_{12})$, a grade-three polynomial was fit to the data of Ref. [35].

Also in this case, within error margins, the iron bulk value is recovered for $x = 0$. The magnitude and the variation with concentration of $B^{\text{eff}}_{[100]}$ for the tetragonal samples is very similar to B_1 of the bulk references. However, this is not the case for the cubic films where only the $x = 0.25$ sample matches the bulk result. For the other two concentrations studied ($x = 0.14$ and 0.15) $B^{\text{eff}}_{[100]}$ does not follow the bulk behavior. Conversely, if we use V_{cell} as the comparing parameter we obtain a better agreement with bulk, as can be observed in Fig. 4(b). It is known that, for bulk $Fe_{1-x}Ga_x$, the change in sign in B_2 occurs at a similar concentration as compared with that of the minimum in B_1. In this sense, our data [shown in Figs. 3(a) and 4(a)] agree with this feature reported for bulk samples [4,5].

A remarkable observation appears when one compares the results obtained for cubic and tetragonal samples: both sets of samples follow the bulk behavior when plotted as a function of V_{cell}. Finally, the similarity between the MEC for the cubic and tetragonal samples supports the application of magnetoelastic energy for cubic system for the description of our samples.

Since B_1 and B_2 are strongly influenced by the local Ga arrangement in the lattice [7,9,10,34,36–38], it is intriguing that experimental results obtained for the tetragonal samples show a similar MEC compared with those of cubic ones. X-ray diffraction measurements [19] indicate that nonrandom solute Ga pairs lead to the development of the B2-like phase probably at less than 10% of Ga content [19]. In tetragonal samples, Ga pairs are preferentially aligned along the growth direction, leading to the measured tetragonal distortion. This specific arrangement of Ga pairs has been proposed as a key factor for the perpendicular magnetic anisotropy (PMA) observed in the tetragonal phase [14], as observed by ferromagnetic resonance measurements and *ab initio* calculations. In Ref. [14], we have shown that the thermal treatment favors the transformation from the tetragonal to the cubic structure, provoking the realignment of the Ga pairs in the equivalent ⟨100⟩ directions. In the case of the tetragonal phase, the estimated amount of Ga pairs along the growth direction is slightly larger than along the other directions (1%). On the other hand, in the cubic films the Ga pairs are equally distributed. Even though magnetic anisotropy is strongly influenced by Ga pairing imbalance, current results indicate that such structural anisotropy does not affect MEC, i.e., cubic and tetragonal magnetoelastic parameters are similar when plotted as a function of the unit-cell volume.

IV. CONCLUSIONS

We have measured MEC in $Fe_{1-x}Ga_x$ thin films grown on ZnSe/GaAs(001), using the magnetoelastic curvature technique, for films with cubic and tetragonal lattice. The main result of this work is that epitaxial thin films present enhanced magnetoelastic coefficients close to those observed in bulk samples. Thus, $Fe_{1-x}Ga_x$ alloy thin films have the potential to be important ingredients for straintronics, spintronics, sensors, and further applications such as acoustic manipulation of magnetic memory elements [39–43].

From a more fundamental point of view, the comparison between bulk samples and out-of-equilibrium grown thin films is fruitful: thin films present a metastable structure due to Ga ordering, i.e., the so-called tetragonal B2 structure, characterized by Ga pairing along the ⟨100⟩ directions. This local atomic arrangement, which is observed in bulk only at very small scales (3 nm inclusions) [44–46], does not affect magnetoelastic coupling in tetragonally distorted thin films, within the experimental accuracy. This leads to the second main result of our article: Ga ordering does not seem to play a decisive role in $Fe_{1-x}Ga_x$ magnetoelasticity. Finally, we discuss the consequences of preferential Ga pairing along the growth direction observed in some of the thin films. Our experimental studies, accompanied by *ab initio* calculations [14], show that a slight imbalance of population of few 10^{-2} between out-of-plane and in-plane directions induces a strong PMA (up to 5×10^5 J/m^3) but it does not seem to significantly affect the $Fe_{1-x}Ga_x$ magnetoelastic coefficients.

ACKNOWLEDGMENTS

J.P. and D.S. gratefully acknowledge partial financial support by the Deutsche Forschungsgemeinschaft (DFG, German Research Foundation) - Projektnummer 31047526 - SFB 762, project B08. ANR under Grant ANR P/180268 "BIOMEN" is gratefully acknowledged by M. Marangolo. J. M. acknowledges partial financial support by PIP 11220120100250CO, PICT 2013-0401, and SIIP 06/C510. The authors acknowledge the staff and responsible persons of the MPBT (physical properties - low temperature) platform of Sorbonne Université for their support.

[1] A. K. Biswas, H. Ahmad, J. Atulasimha, and S. Bandyopadhyay, Nano Lett. **17**, 3478 (2017).
[2] J. Cui, J. L. Hockel, P. K. Nordeen, D. M. Pisani, C.-Y. Liang, G. P. Carman, and C. S. Lynch, Appl. Phys. Lett. **103**, 232905 (2013).
[3] C.-W. Nan, M. I. Bichurin, S. Dong, D. Viehland, and G. Srinivasan, Appl. Phys. Lett. **103**, 232905 (2013).
[4] A. E. Clark, K. B. Hathaway, M. Wun-Fogle, J. B. Restorff, T. A. Lograsso, V. M. Keppens, G. Petculescu, and R. A. Taylor, J. Appl. Phys. **93**, 8621 (2003).
[5] A. E. Clark, J. B. Restorff, M. Wun-Fogle, T. A. Lograsso, and D. L. Schlagel, IEEE Trans. Magn. **36**, 3238 (2000).
[6] H. Cao, P. M. Gehring, C. P. Devreugd, J. A. Rodriguez-Rivera, J. Li, and D. Viehland, Phys. Rev. Lett. **102**, 127201 (2009).
[7] M. Laver, C. Mudivarthi, J. R. Cullen, A. B. Flatau, W. C. Chen, S. M. Watson, and M. Wuttig, Phys. Rev. Lett. **105**, 027202 (2010).
[8] J. Boisse, H. Zapolsky, and A. Khachaturyan, Acta Mater. **59**, 2656 (2011).
[9] H. Wang, Y. N. Zhang, R. Q. Wu, L. Z. Sun, D. S. Xu, and Z. D. Zhang, Sci. Rep. **3**, 3521 (2013).
[10] Y. Zhang and R. Wu, IEEE Trans. Magn. **47**, 4044 (2011).
[11] Y. N. Zhang, J. X. Cao, and R. Q. Wu, Appl. Phys. Lett. **96**, 023513 (2010).
[12] Y. Zhang, R. Q. Wu, H. M. Schurter, and A. B. Flatau, J. Appl. Phys. **108**, 023513 (2010).
[13] R. Q. Wu, J. Appl. Phys. **91**, 7358 (2002).
[14] M. Barturen, J. Milano, M. Vásquez-Mansilla, C. Helman, M. A. Barral, A. M. Llois, M. Eddrief, and M. Marangolo, Phys. Rev. B **92**, 054418 (2015).
[15] E. du Trémolet de Lacheisserie and J. C. Peuzin, J. Magn. Magn. Mater. **136**, 189 (1994).
[16] D. Sander, Rep. Prog. Phys. **62**, 809 (1999).
[17] E. du Trémolet de Lacheisserie, *Magnetostriction: Theory and Applications of Magnetoelasticity* (CRC Press, Boca Raton, 1993).
[18] C. Kittel, Rev. Mod. Phys. **21**, 541 (1949).
[19] M. Eddrief, Y. Zheng, S. Hidki, B. Rache Salles, J. Milano, V. H. Etgens, and M. Marangolo, Phys. Rev. B **84**, 161410(R) (2011).
[20] M. Barturen, B. Rache Salles, P. Schio, J. Milano, A. Butera, S. Bustingorry, C. Ramos, A. J. A. De Oliveira, M. Eddrief, E. Lacaze, F. Gendron, V. H. Etgens, and M. Marangolo, Appl. Phys. Lett. **101**, 092404 (2012).

[21] M. Barturen, M. Sacchi, M. Eddrief, J. Milano, S. Bustingorry, H. Popescu, N. Jaouen, F. Sirotti, and M. Marangolo, Eur. Phys. J. B **86**, 191 (2013).
[22] S. Tacchi, S. Fin, G. Carlotti, G. Gubbiotti, M. Madami, M. Barturen, M. Marangolo, M. Eddrief, D. Bisero, A. Rettori, and M. G. Pini, Phys. Rev. B **89**, 024411 (2014).
[23] K. Dahmen, H. Ibach, D. Sander, J. Magn. Magn. Mater. **231**, 74 (2001).
[24] D. Sander and J. Kirschner, Phys. Status Solidi B **248**, 2389 (2011).
[25] D. E. Parkes, L. R. Shelford, P. Wadley, V. Holý, M. Wang, A. T. Hindmarch, G. Van Der Laan, R. P. Campion, K. W. Edmonds, S. A. Cavill, and A. W. Rushforth, Sci. Rep. **3**, 2220 (2013).
[26] M. Eddrief, M. Marangolo, S. Corlevi, G. Guichar, V. H. Etgens, R. Mattana, D. H. Mosca, and F. Sirotti, Appl. Phys. Lett. **81**, 4553 (2002).
[27] M. Eddrief, M. Marangolo, V. H. Etgens, S. Ustaze, F. Sirotti, M. Mulazzi, G. Panaccione, D. H. Mosca, B. Lépine, and P. Schieffer, Phys. Rev. B **73**, 115315 (2006).
[28] K. Dahmen, S. Lehwald, and H. Ibach, Surf. Sci. **446**, 161 (2000).
[29] D. Sander, J. Phys.: Condens. Matter **16**, R603 (2004).
[30] D. Sander, Z. Tian, and J. Kirschner, J. Phys.: Condens. Matter **21**, 134015 (2009).
[31] W. A. Brantley, J. Appl. Phys. **44**, 534 (1973).
[32] V. Z. C. Paes and D. H. Mosca, J. Appl. Phys. **112**, 103920 (2012).
[33] J. B. Restorff, M. Wun-Fogle, K. B. Hathaway, A. E. Clark, T. A. Lograsso, and G. Petculescu, J. Appl. Phys. **111**, 023905 (2012).
[34] J. R. Hattrick-Simpers, D. Hunter, C. M. Craciunescu, K. S. Jang, M. Murakami, J. Cullen, M. Wuttig, I. Takeuchi, S. E. Lofland, L. Benderksy, N. Woo, R. B. V. Dover, T. Takahashi, and Y. Furuya, Appl. Phys. Lett. **93**, 102507 (2008).
[35] R. Kellogg, A. Russell, T. Lograsso, A. Flatau, A. Clark, and M. Wun-Fogle, Acta Mater. **52**, 5043 (2004).
[36] J. Cullen, P. Zhao, and M. Wuttig, J. Appl. Phys. **101**, 123922 (2007).
[37] S. C. Hong, W. S. Yun, and R. Wu, Phys. Rev. B **79**, 054419 (2009).
[38] H. Wang, Y. N. Zhang, T. Yang, Z. D. Zhang, L. Z. Sun, and R. Q. Wu, Appl. Phys. Lett. **97**, 262505 (2010).
[39] L. Thevenard, C. Gourdon, J. Y. Prieur, H. J. von Bardeleben, S. Vincent, L. Becerra, L. Largeau, and J.-Y. Duquesne, Phys. Rev. B **90**, 094401 (2014).
[40] H. Riahi, L. Thevenard, M. Maaref, B. Gallas, A. Lemaître, and C. Gourdon, J. Magn. Magn. Mater. **395**, 340 (2015).
[41] L. Thevenard, I. S. Camara, J.-Y. Prieur, P. Rovillain, A. Lemaître, C. Gourdon, and J.-Y. Duquesne, Phys. Rev. B **93**, 140405(R) (2016).
[42] L. Thevenard, I. S. Camara, S. Majrab, M. Bernard, P. Rovillain, A. Lemaître, C. Gourdon, and J.-Y. Duquesne, Phys. Rev. B **93**, 134430 (2016).
[43] S. Davis, A. Baruth, and S. Adenwalla, Appl. Phys. Lett. **97**, 232507 (2010).
[44] Y. He, C. Jiang, W. Wu, B. Wang, H. Duan, H. Wang, T. Zhang, J. Wang, J. Liu, Z. Zhang, P. Stamenov, J. M. D. Coey, and H. Xu, Acta Mater. **109**, 177 (2016).
[45] J. Premper, D. Sander, and J. Kirschner, Rev. Sci. Instrum. **83**, 073904 (2012).
[46] N. Srisukhumbowornchai and S. Guruswamy, J. Appl. Phys. **90**, 5680 (2001).